Drip irrigation frequency leads to plasticity in root water uptake by apple trees

Stefano Brighenti, Massimo Tagliavini, Francesco Comiti, Agnese Aguzzoni, Nicola Giuliani, Ahmed Ben Abdelkader, Daniele Penna, Damiano Zanotelli

Agricultural Water Management 298 (2024) 108870

Contents lists available at ScienceDirect

Agricultural Water Management

journal homepage: www.elsevier.com/locate/agwat

Drip irrigation frequency leads to plasticity in root water uptake by apple trees

Stefano Brighenti [a,b,*], Massimo Tagliavini [a], Francesco Comiti [a,c], Agnese Aguzzoni [d], Nicola Giuliani [a], Ahmed Ben Abdelkader [a,e], Daniele Penna [f,g], Damiano Zanotelli [a]

[a] Faculty of Agricultural, Environmental and Food Sciences, Free University of Bozen, Bolzano, Italy
[b] Competence Centre for Mountain Innovation Ecosystems, Free University of Bozen, Bolzano, Italy
[c] Department of Land, Environment, Agriculture and Forestry, University of Padova, Italy
[d] Eco Research, Bozen, Bolzano, Italy
[e] INRAE-UR1115 (PSH), Site Agroparc, Avignon, France
[f] Department of Agriculture, Food, Environment and Forestry, University of Firenze, Firenze, Italy
[g] Oregon State University, Forest Engineering Resources and Management Department, Corvallis, OR, USA

ARTICLE INFO

Keywords:
Ecohydrology
Precision irrigation
Critical zone

ABSTRACT

Stable isotopes of hydrogen and oxygen are used in agriculture to investigate the water sources used by crops. Yet, isotopic research on irrigated orchards is still scarce. We investigated the isotopic variability in an apple tree plantation in the Eastern Italian Alps (South Tyrol) during the growing seasons 2020 and 2021. The orchard was subject to an irrigation trial, whereby a drip system was triggered at different soil water potential thresholds at two treatment types: full irrigation (FI, −30 kPa) and deficit irrigation (DI, −60 kPa). On a bi-weekly basis, we sampled precipitation, river water, and groundwater used for irrigation. At both FI and DI, we sampled soil at different depths and bark-devoid branches, and cryogenically extracted their water. Isotopic analyses revealed large differences in $\delta^{18}O$ values of soil water belonging to the two irrigation treatments, particularly during the irrigation period (up to 8.9‰). In xylem water, the differences were much smaller (up to 1.6‰). Mixing models (EEMMA) estimated a larger groundwater (vs. rainwater) fraction in the shallow soil (5–10 cm) at FI (25–55%) than at DI (0–5%), compatible with a larger presence of irrigation water in the former. DI plants had a deeper root water uptake (32.0 ± 11.9 cm) than FI ones (19.3 ± 14.5 cm) during the irrigation period. This agreed with the results of mixing models (IsoSource) that estimated a larger use of deeper (60–65 cm) soil water (42 ± 18%) and a lower use of shallow soil water (13 ± 6%) for DI than for FI (34 ± 26% and 27 ± 26%) during the same period. This root water uptake plasticity explains the lacking evidence of physiological stress in sap flux records at DI and supports the potential for further improvements of precision irrigation in similar climatic and edaphic settings.

1. Introduction

Agriculture is by far the most water intensive human activity (FAO, 2020). Globally, about 60% of the water provided to the cultivations and not returned to aquatic systems is managed in an unsustainable way, and may be reduced to meet local-scale water scarcity (Mekonnen and Hoekstra, 2020). Since the water used for irrigation is withdrawn from the environment (soil, groundwater, streams), and/or may be allocated to other human sectors, a precise and balanced use of irrigation water is essential to ensure both crop production and environmental/social needs (Pastor et al., 2019). This is particularly important within the ongoing climatic changes, posing challenges for the environmental sustainability of crop production under a declining availability of water resources (World Bank, 2022). In this context, precision irrigation offers powerful tools to reduce the exploitation of water resources while maintaining optimal crop yields (Liang et al., 2020). Stable isotopes in the water molecule (^{18}O and ^{2}H) are widely used as natural tracers to investigate the ground-plant-atmosphere interactions within the critical zone (Beyer and Penna, 2021; Brooks et al., 2015; Sprenger et al., 2016; Kirchner et al., 2023), and are a valuable tool to understand the use of water by plants also in agriculture (Penna et al., 2020). Isotope-based studies can help estimating the relative importance of different soil

* Correspondence to: Piazza dell'Università 5, Bolzano, 39100 Italy.
E-mail address: stefano.brighenti@unibz.it (S. Brighenti).

https://doi.org/10.1016/j.agwat.2024.108870
Received 11 March 2024; Received in revised form 3 May 2024; Accepted 6 May 2024
Available online 16 May 2024
0378-3774/

depths for root water uptake (Wang et al., 2018; 2020; Shi et al., 2023a; 2022; Zhao et al., 2022), including rock moisture (Wang et al., 2023; Li et al., 2024), and can inform water management (Ma and Song, 2019; Penna et al., 2020) and help identify the most waterwise irrigation supply (Cao et al., 2018; Wu et al., 2018; Li et al., 2019; Canet-Martí et al., 2023). While studies on the use of irrigation by crops were mostly focused on herbaceous plants such as maize, wheat, rice, or cotton (e.g., Ma and Song, 2016; 2019; Mahindawansha et al., 2018; Wu et al., 2018; Goebel and Lascano, 2019; Liu et al., 2021; Wang et al., 2023), research on woody plantations has been increasing during the last decade (Lauteri et al., 2005; Sun et al., 2011; Cao et al., 2018; Zheng et al., 2018; Li et al., 2019; Liu et al., 2019; Penna et al., 2021; Aguzzoni et al., 2022; Giuliani et al., 2023). Some of these studies aimed at finding an optimal irrigation strategy in areas of water scarcity. For instance, in semi-arid Central/Eastern China, different irrigation techniques were related to water uptake from different depths in cherry (Li et al., 2019) and apple (Zheng et al., 2018) trees. For the latter, isotopic evidence of a prevalent use of shallow soil water by apple trees allowed addressing irrigation improvements by providing water to the topsoil (Zheng et al., 2018). While these studies investigated how water from different soil depths is tapped by trees, understanding the relative contribution from irrigation to xylem water can be challenging. In two apple orchards of a continental mountain valley (Eastern Italian Alps), Penna et al. (2021) found a prevalent use of water from intermediate depths (20–40 cm) but could not find isotopic evidence of (sprinkling) irrigation water use by apple trees. The authors attributed this lack of evidence to the strong evaporative fractionation occurring within the soil, coupled with efficient mixing of old and new water, disrupting the isotopic fingerprint of the irrigation input (Penna et al., 2021). Indeed, both isotopic fractionation and dilution with subsequent precipitation events can strongly modify the original signature of the water infiltrating into the soil (Sprenger et al., 2016). This phenomenon might be more evident in humid climates and/or where irrigation is supplied with precision systems, where rain events can efficiently dampen an irrigation fingerprint already smoothened within the soil by relatively low supplies. Moreover, groundwater is often used for irrigation (Siebert et al., 2010), and the consequent isotopic overlapping of their signatures (Cao et al., 2018) hinders any estimation of the groundwater and irrigation fractions in the soil water. As further complication, the progressive depletion in heavy isotopes often occurring with depth can make water from the deeper soil isotopically very similar to groundwater, when compared with water from the shallow soil, especially under the raise of capillary fringe (Sprenger et al., 2016). Despite these limitations, in a cherry tree orchard of Central/Eastern China, Cao et al. (2018) could find different irrigation water uses from trees with contrasting drip irrigation supply (70%, 85% and 100% of the design irrigation quota). Different isotopic conditions in soil and xylem water were found in different treatments. During the fruit growth stage, fully irrigated trees had the largest fraction of irrigation water (25–32%) in their xylem water, when compared with intermediate (14–27%) and least irrigated trees (11–16%; Cao et al., 2018). Despite evidence of root water uptake plasticity to irrigation deficit, we are not aware of any study investigating how contrasting water supply affects root water uptake in apple trees in temperate climates.

For this reason, we investigated the ecohydrological dynamics of an apple orchard in South Tyrol (Etsch/Adige valley, Northern Italy) during two consecutive growing seasons (2020–2021). In the orchard, drip irrigation (tapped from a well) was triggered at different soil water potentials (-30 kPa for full irrigation - FI, −60 kPa for deficit irrigation - DI) at different blocks of trees. We estimated the isotopic composition of irrigation (i.e., groundwater), rainwater, soil, and xylem water to address the following research hypotheses related to the irrigation period:

- Since the irrigation supply was different in the two treatments, the soil and the xylem water was isotopically different between the two treatment types;
- These differences can be related to a contrasting contribution of groundwater (vs. rainwater), which was higher at FI than at DI due to higher irrigation supply in the former;
- Since less water was available in the shallow soil at DI, apple trees tapped water from a deeper soil than at FI.

2. Materials and methods

2.1. Study area

The study was carried out in 2020 and 2021, in a mature apple tree orchard (cv. Nicoter on M9 rootstock) named Binnenland, located in a flat area of the Etsch/Adige floodplain (South Tyrol, Eastern Italian Alps; Fig. 1) at 221 m a.s.l. The orchard was established in 2007 with planting distances of 3.0 * 0.8 m (4167 trees ha^{-1}), and the tree height was ca. 3.5 m. The trees were protected against hail by a net. Details about tree productivity are given in Ben Abdelkader et al. (2022).

The climate of the area is temperate, without dry seasons and with warm summers (Cfb, according to Köppen classification). The long-term series (1983–2022) at the closest automatic weather station (AWS) of Auer/Ora (46.35°N, 11.31°W) shows a mean annual air temperature of 12.8°C, and a mean total annual precipitation of 821 mm (Autonomous Province of Bozen-Bolzano APB, 2023). The plot was located 90–160 m from the Etsch river, suggesting horizontal exchanges with the groundwater table. However, long-term monitoring with piezometers at a depth of 2.3 m never revealed groundwater presence during the period 2019–2021 (Giuliani et al., 2023).

The soil had a sandy loam texture, with an average of 58% of sand and 39% of silt and 3% of clay, and a bulk density (0–60 cm depth) of 1.37 ± 0.12 kg L^{-1} (Giuliani et al., 2023; Zanotelli et al., 2022). At 0–40 cm depth, average pH was 7.2 and the soil organic matter was 2.1%.

The crop was managed according to the integrated fruit production guidelines. A 0.8 m wide soil strip centred in the tree rows was maintained free of weeds through herbicides, whereas spontaneous herbaceous vegetation was allowed to grow in the orchard alleys.

2.2. Irrigation treatments

Starting from 2019, the plot hosted a field trial involving the use of different irrigation treatments, distributed according to a randomised block design with four blocks. Each experimental unit consisted of ten adjacent trees (Ben Abdelkader et al., 2022). We selected four blocks subjected to two of these treatments, representing contrasting soil water potential thresholds used to trigger the irrigation, −30 kPa for full irrigation (FI), and −60 kPa for deficit irrigation (DI). Two drip lines laying on the soil surface, each of them stretching along the tree row, 40 cm from each other, were deployed. Each tree was irrigated by four (40 cm spaced) drippers, providing water with 2.3 L hr^{-1} each. Soil water potential (SWP) was recorded at hourly scale by Arduino-monitored, self-made tensiometers (Thalheimer, 2013), having an operation range within 0 and −80 kPa. Two tensiometers per treatment were installed in one replicate block at 10 cm distance from the dripper and at 25 cm soil depth. Irrigation was automatically triggered whenever the two predefined SWP thresholds were reached by at least one of the two tensiometers. Each irrigation event lasted 120 and 180 minutes at FI and DI, respectively, to bring back the soil moisture to the field capacity. Irrigation started on 29th of May 2020 and 4th of June 2021, and ended on 25th of August 2020 and 12th of September 2021 (Table 1). Although the total rainfall amount in 2021 was lower than in 2020, it was more homogeneously distributed throughout the season than in 2020. This fact, associated with a lower air temperature in 2021 than in 2020, reduced the need and the number of irrigation events

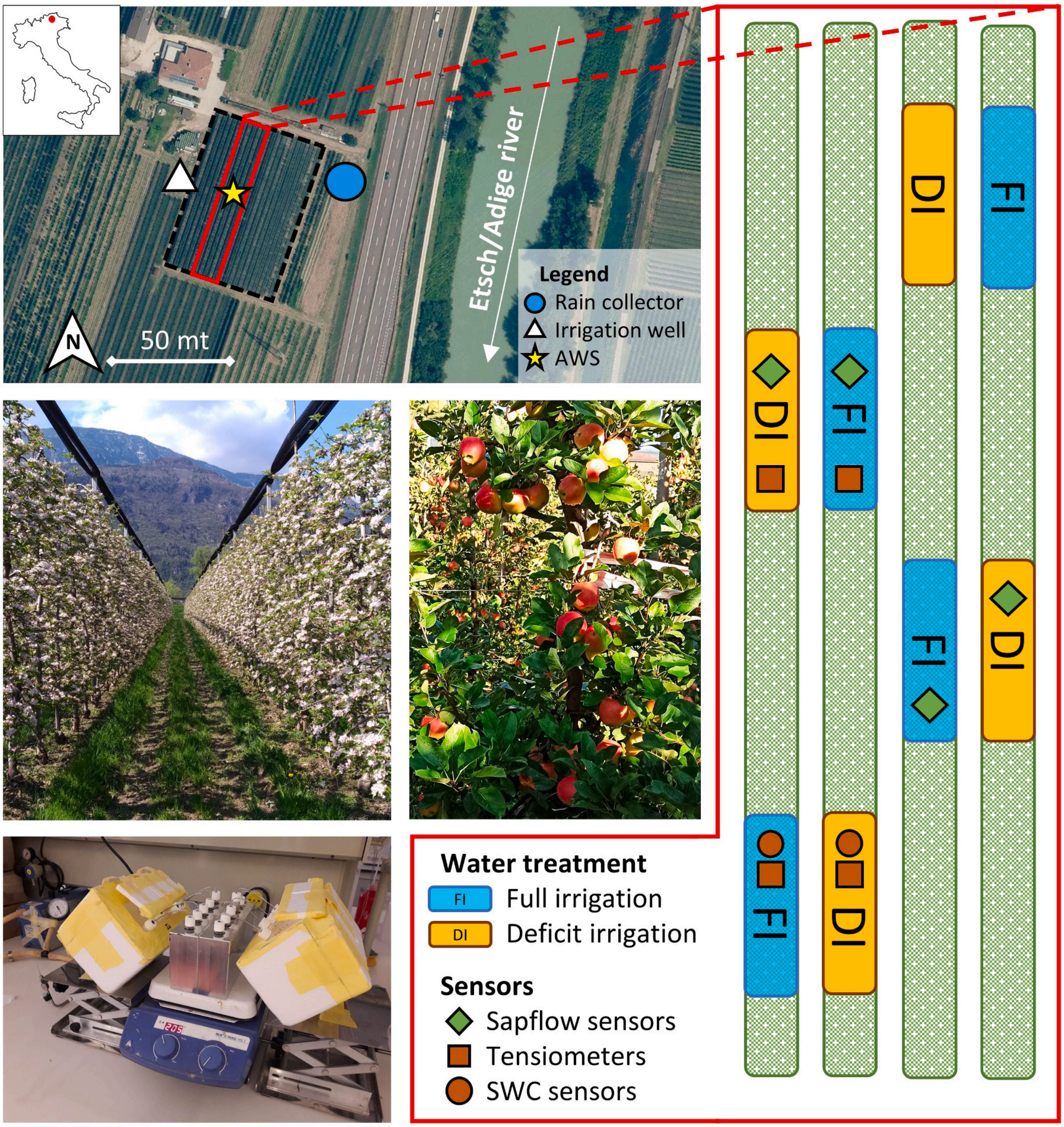

Fig. 1. The investigated orchard, Binnenland. Upper part: location of the study area in Italy, and summary of the main ecohydrological features. The close-up represents the monitored rows, with the experimental blocks and their irrigation treatments. Pictures represent the orchard during flowering and fruit harvest (middle), and the cryogenic vacuum distillation system at the Free University of Bozen/Bolzano (bottom).

Table 1
Summary statistics of the meteorological conditions and irrigation supply at Binnenland during May-October 2020 and 2021. As reference, the historical series (1983–2022) at the AWS of Auer/Ora have an average of 19.4°C for air temperature and 526 mm of cumulative precipitation, during the same months.

Parameter	2020	2021
Daily air temperature (°C; mean ± st.dev.)	19.0 ± 4.8	18.1 ± 4.9
Cumulative precipitation (mm)	593	442
Irrigation period	29/5–4/9	4/6–22/9
FI irrigation events (n) - supply (m^3 ha^{-1})	17* - 835	7–536
DI irrigation events (n) - supply (m^3 ha^{-1})	3* - 145	2–230

* During the period 25th of June - 10th of July 2020, there was a partial clogging of irrigation filters. Before the maintenance intervention, 7 irrigation events at FI and 2 events at DI supplied water at a low rate (0.6 L hr^{-1}) instead of 2.3 L hr^{-1}.

(Table 1).

2.3. Field monitoring and sampling

To estimate the root distribution within the soil, in winter 2018/2019 (i.e., before the start of the field trial), soil cores were sampled at different depths (every 10 cm along the 0–80 cm soil layer), and at distances of 25 cm and 45 cm from the trunk over three radial distances from the row (0°, 45°, 90°). This operation was repeated for three trees.

The main field activities were conducted from May 2020 to November 2021, with fortnightly visits during the growing season.

Soil water potential (SWP, -kPa) was recorded by tensiometers as described above. Additionally, TMS-4 soil probes (Tomst Ltd., Czech Republic) were installed to record volumetric moisture (electromagnetic Time Domain Transmissions) at 15 min resolution. These sensors were used to obtain continuous data of soil water content (SWC, m^3 m^{-3}). They were placed at 20 cm and 40 cm depths below the canopy of two blocks belonging to the FI and DI treatments, and coupled with tensiometers located at 30 cm depth (Fig. 1). The xylem sap flow velocities were measured with SFM1 sensors (ICT International, Armidale, NSW, Australia), using the heat ratio method. Each sensor, consisting of a set of three needles, has two couples of thermistors on the needles, allowing for two measuring points within the xylem. Two SFM1 sensors were installed in June 2020 on one tree per treatment, while two additional sensors were installed in March 2021 on trees (one per treatment) of a different block. Suction cups were installed at 10, 20 and 60 cm, at two opposite FI and DI blocks, and were used during each sampling campaign to extract gravity-driven soil water. The cups only worked on a few occasions (19 of 174 total attempts).

An evaporation-free rain collector (Palmex ltd, Zagreb, Croatia) that limits kinetic isotope fractionation (Gröning et al., 2012) was installed to collect precipitation in an open area (Fig. 1). Four additional HDPE containers with funnels were installed beneath trees to gather throughfall, and one stemflow collector was attached to one plant belonging to the treatment FI. All containers were emptied during each field visit (on a bi-weekly basis), after the collection of water samples in 50 PPE bottles with double caps. During each sampling, the same type of container was used to collect river water and groundwater at the well tapped for irrigation supply, at a faucet located in the joint of the irrigation pipe into the well (Fig. 1).

During each field campaign, we used a gravity corer to sample soil samples at different depth intervals (5–10 cm, 10–15 cm, 25–30 cm, 60–65 cm). Soil samples were collected at two random locations (changing among samplings) belonging to the investigated FI and DI blocks, with coring undertaken within the soil strip close to the centre of the tree row (< 30 cm). Each sample was collected in three replicates, and placed in 12 mL Exetainer® borosilicate containers with pierceable caps. Twigs from the four blocks were collected from apple trees at breast height (1.4 m) and placed in Exetainers® after their bark was removed (Landgraf et al., 2022). During each field campaign, two different trees from the same irrigation treatment unit (avoiding border trees) were sampled, with two samples per tree collected. This hindered a stress related to a complete removal of above ground organs from few single trees, and the associated (damage to plants and) potential modification of the xylem isotopic signature. Samples were placed in thermal bags (< 6°C) immediately after their collection, and taken to the laboratory where they were stored at 4°C until processing. The time elapsed between the sampling and the latest irrigation event spanned from one hour to eight months at both treatments, and the time elapsed between the sampling and the latest rainfall event spanned from one to 21 days.

2.4. Laboratory activities

Laboratory activities were undertaken at the Faculty of Science and Technology of the Free University of Bozen/Bolzano, Italy. To estimate the root density, coarse (Ø > 2 mm) and fine (Ø < 2 mm) roots were sorted from each soil sample, rinsed with tap water, separately dried in a ventilated oven (65°C, 72 h), and then weighed (see Frasier et al., 2016). Density of fine and coarse roots (g L^{-1}) was calculated based on the section of the corer, approximated to a cylinder (150.28 cm^3). For each soil depth interval, we calculated the fine roots recovery rate, i.e., the percentage of samples where fine roots density was larger than zero.

We used the Cryogenic Vacuum Distillation (CVD) technique (Koeniger et al., 2011) to extract water from the soil (soil water) and the bark-devoid twigs (xylem water), following the same instruments, procedure, heating temperature (205°C) and extraction times (15 min) described in Zuecco et al. (2022). Exetainer® vials (Labco Ltd., UK) were weighed before (tare) and after the sampling, and after CVD to estimate the extraction efficiency (R_{eff}) based on weight after 48 h in the oven (105°C; Zuecco et al., 2022). We only analysed water samples associated with R_{eff} > 98%, and extraction was repeated on sample replicates if this minimum efficiency was not achieved. Overall, R_{eff} for the analysed samples was 98.9 ± 0.9% for twigs, and 99.6 ± 0.4% for soils.

The isotopic composition of soil, precipitation, river water, and groundwater was determined with a laser spectrometer (CRDS Picarro L2130i, CA, USA). The precision of the analyser was 0.5‰ for δ^2H, and 0.25‰ for δ^{18}O. Memory effect (Cui et al., 2017) was minimised following the procedure reported in Penna et al. (2012). Xylem water was analysed with isotope-ratio mass spectrometry (IRMS Delta V Advantage Conflo IV, Thermo Fisher Scientific Inc., Waltham, Massachusetts, USA), with a precision of 2.5‰ for δ^2H, and 0.2‰ for δ^{18}O. All isotopic results are referred to the VSMOW (Vienna Standard Mean Ocean Water) and expressed in ‰ notation. The comparison between IRMS and CRDS on 19 samples (internal standards and throughfall water samples) showed an absolute difference and standard error of 0.27 ± 0.51‰ for δ^2H and 0.02 ± 0.06‰ for δ^{18}O.

2.5. Processing of field data

We retrieved meteorological data from the AWS (Fig. 1) installed by Zanotelli et al. (2022) in the orchard (2020–2021), recording air temperature (°C), precipitation (mm), and photosynthetic active radiation (PAR; mol m^{-2} d^{-1}) and aggregated them to daily steps. We converted the electromagnetic data obtained with TMS-4 probes in Volumetric Water Content (%) using calibration curves obtained in the laboratory.

The volumetric value of the sap flow (T_{sap}, cm^3 h^{-1}) was obtained as the sum of the two corrected sap velocities (cm h^{-1}) measured every 15 minutes, multiplied by the respective fraction of trunk cross-sectional area (cm^2, see Zanotelli et al., 2022). The total conductive area was 14.9 ± 1.5 cm^2 of which 84% was attributed on average to the external sensor and 16% to the inner one. Given the uncertainties on the absolute flux values and their dependence on installation and tree specific characteristics, all sap flow data were normalised (0–100%) considering the record during which transpiration occurred under optimal conditions within both treatments. Accordingly, all data were normalised considering that record as 100% sap flux velocity.

Based on the irrigation records, we distinguished for each year an “irrigation” and a “non-irrigation” period. The former encompassed the sampling dates between the first irrigation, and ten days after the last irrigation event in the field. The latter included all other dates from May to October.

2.6. Analysis of isotopic data

The isotopic offset between the samples and the Local Meteoric Water Line (Rozanski et al., 1993) was calculated as line-conditioned excess (Lc-excess; Dansgaard, 1964), and corrected following the procedure outlined by Zuecco et al. (2022) to account for the instrumental uncertainties of the IRMS. Accordingly, the Lc-excess (Landwehr and Coplen, 2006) was divided by a coefficient of uncertainty *S*, based on the instrumental standard deviation of both isotopes and the slope of the LMWL.

To estimate the relative differences of isotopic conditions between the two irrigation treatments, we calculated for each date and water pool (soil depth interval, xylem water) the index of isotopic difference (δISO), defined as:

$$\delta ISO = \delta^{18}O_{FI} - \delta^{18}O_{DI}$$

where $\delta^{18}O_{FI}$ and $\delta^{18}O_{DI}$ are the isotopic values of soil/xylem water for the FI and DI, respectively. For xylem water, δISO was calculated as the average of all pairwise FI-DI comparisons. Positive δISO indicates FI sample more enriched in heavy isotopes than its DI counterpart (i.e., soil depth interval or xylem water), and negative δISO indicates FI more depleted than its DI counterpart.

2.7. End-member mixing analyses and depth of root water uptake

Based on δ^{18}O measurements (less prone to fractionation than δ^2H), we estimated the relative contribution of groundwater (F_{gw}) and rain water (F_{rw}) to soil water at different depths in the two treatments, and to xylem water of trees belonging to different blocks. Then, we estimated the relative contribution of water from different soil depth intervals to xylem water fluxes (F_{sd}). We performed the first analysis with a novel method developed by Kirchner (2023). The Ensemble End-Member Mixing Analysis (EEMMA) uses the tracer time series to cope with the shortcomings typically encountered in mixing models, such as overlapping means of different end-members, memory effects of mixtures, missing/unsampled end-members, and sharp temporal fluctuations of the isotopic signatures. Since the outcomes of EEMMA are summary statistics for the end-member contribution, we performed the analyses only for the irrigation period. EEMMA was performed with the package EEMMA (Kirchner, 2023) in R (R R Core Team, 2021), and based on a day of the year (DOY) ordination to increase the number of points in the series. For each mixture (soil water at each depth interval and xylem water, at different blocks), we used models without accounting for an unsampled end-member and memory effect in the mixture. Then, we repeated the analyses including these parameters, to estimate their significance (Kirchner, 2023).

We used a graphical/mathematical method to calculate the average depth of root water uptake (Z_{rwu}, cm). This method examines the isotopic gradient ($\delta^{18}O$ or $\delta^{2}H$) occurring in the vertical profile of the soil to identify the depth at which the isotopic signature of xylem water meets that of the soil water (Wang et al., 2010; Cao et al., 2018). The isotopic gradient was calculated based on $\delta^{18}O$, by rescaling depth intervals to average depth (e.g., 5–10 cm depth was rescaled to 7.5 cm), and using polynomial (n = 3) fitting to model the isotopic values of the range between two depths.

Then, we calculated the contribution from different soil depth intervals (F_{sd}) to xylem water (mixture) during each date and at each irrigation treatment. We used end-member mixing models (EMMA) with IsoSource (v 1.3.1; Philipps and Gregg, 2003), a widely used method allowing to account for multiple sources using only one tracer. The software solves mathematical solutions of several end-members by considering all possible combinations (given a provided increment value) of end-member contributions. The output is a range of feasible combinations that the software provides for each end-member, under a certain tolerance. We used a tolerance of 0.01‰ and an increment of 1‰. IsoSource was performed separately for each xylem water sample, considering treatment-specific (DI and FI) end-member values (water from different depth intervals). Results are reported as average and standard deviation values.

2.8. Additional statistical analyses

We analysed differences in isotopic composition, Z_{rwu}, and F_{sd} between groups (period, year, soil depth, irrigation treatment) and their combinations based on nonparametric pairwise comparisons with the Wilcoxon test (non-normal distribution and/or heteroscedasticity maintained even after transformation). We estimated correlations between variable pairs (SWP, Z_{rwu}, F_{sd}) with two-tailed Spearman rank (ρ coefficient) or Pearson correlation (r coefficient), depending on the non-normal or normal distribution of the data, respectively (SPSS Statistics

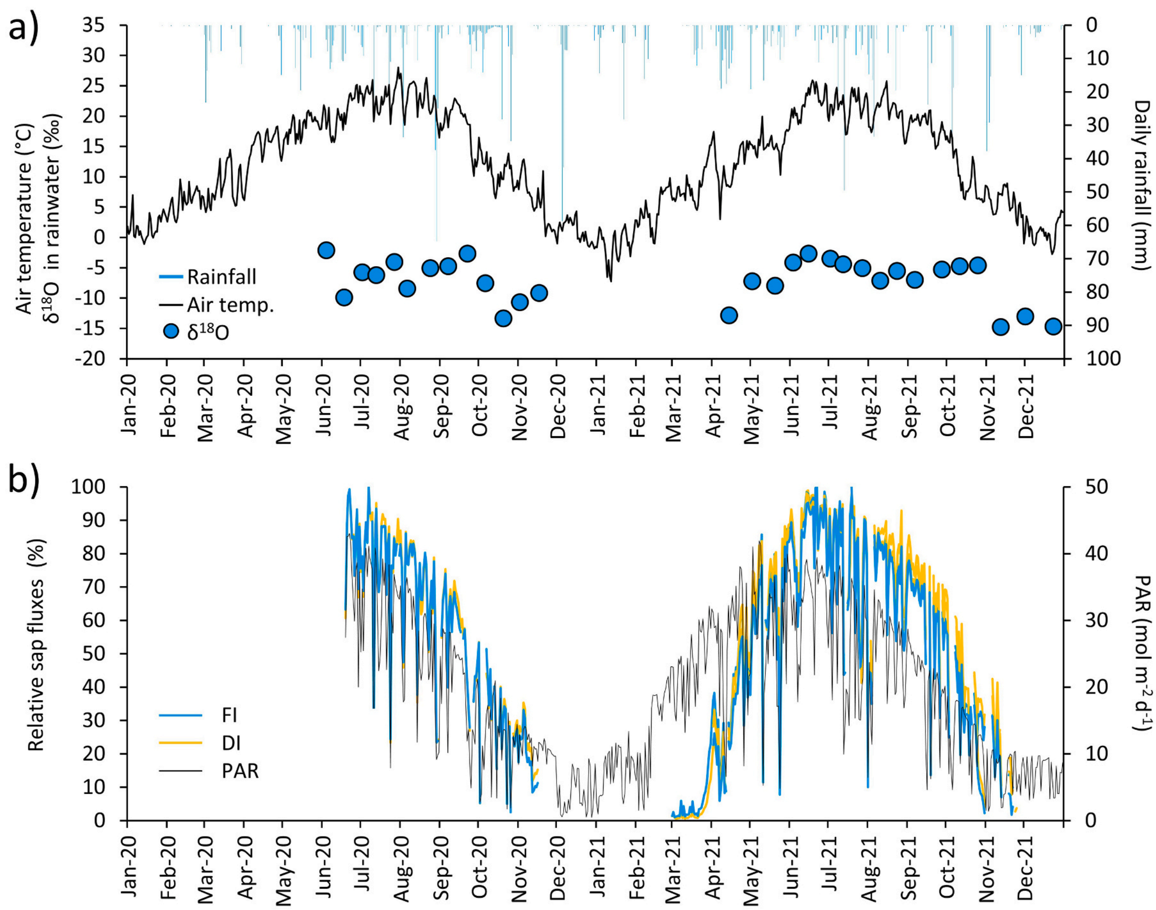

Fig. 2. Time series of meteorological and sapflow records. a) Daily air temperature and precipitation during 2020 and 2021, and values of $\delta^{18}O$ in the collected samples of precipitation. NOTE: data of precipitation and air temperature belonging the period 1/1–18/6/20 refer to the closest meteorological station of the Autonomous Province of Bozen/Bolzano (Auer/Ora, 257 m a.s.l.; 2 km air distance from Binnenland); b) Average daily photosynthetic active radiation (PAR) and relative sap fluxes for DI and FI trees.

software, v.27; IBM, 2018).

3. Results

3.1. Meteorological conditions, soil moisture and sap fluxes

During the period from May to October, the mean daily air temperature and cumulative precipitation were higher in 2020 than in 2021 (Fig. 2a; Table 1, Supplementary 1).

The records of soil water content (SWC) and water potential (SWP) highlighted different temporal patterns for the two treatments (Fig. 3). There was a transient rise in SWC and SWP immediately after rainfall and irrigation events, which were better recorded at 20 cm. Because of the few irrigation events, the SWC steadily declined at DI starting from May, while multiple irrigation events at FI maintained a rather stable SWC (Fig. 3). Relatively intense rain events (40–60 mm), capable of boosting up the SWC and SWP at all depths (particularly at DI), occurred during late August 2020 and early July 2021 (Fig. 3). For this reason, in both treatments, a lower number of irrigation events took place in summer 2021 when compared with 2020 (Table 1). While during summer 2020 irrigation was applied throughout summer (at least at FI), water supply ceased during the first decade of July during 2021 until the 12th of September, when one irrigation event occurred only in FI (Fig. 3).

Sap flux density records did not reveal differences between DI and FI (Fig. 2b; see also Zanotelli et al., 2022). Indeed, we found a strong positive correlation ($p < 0.001$) in both FI ($r = 0.91$) and DI ($r = 0.92$) treatments between the relative sap fluxes (%) and the PAR during the growing season (Fig. 2b; Supplementary 2).

3.2. Root density patterns

We found higher density (median value 0.08 g L^{-1}) and recovery rates (88.9%) in the upper part of the soil profile (0–40 cm) when compared with the deeper layers (0.01 g L^{-1}, 69.0% at 40–80 cm). The largest median density (0.25 g L^{-1}) and recovery rate (100%) were found at 10–20 cm, and declined towards shallower and deeper soil intervals (Fig. 4). Unexpectedly, the 40–50 cm depth interval had the lowest recovery rate (32.4%) of fine roots.

3.3. Isotopic conditions of different water pools

When plotted in a dual isotope scatterplot ($\delta^{18}O$ - $\delta^{2}H$), samples from precipitation ($n = 40$) defined a local meteoric water line (LMWL) to which throughfall ($n = 57$), stemflow ($n = 27$), groundwater ($n = 41$), and river water ($n = 31$) samples aligned (Fig. 5a). Samples from soil ($n = 249$) and xylem ($n = 163$) water had a large isotopic variability, while those from groundwater (used for irrigation) and river water were consistently more depleted in heavy isotopes, with little variability (Fig. 5a; Fig. 6a). There was a tendency towards lower $\delta^{18}O$ of soil water when moving deeper into the soil, with this trend being more evident at DI than at FI (Fig. 6b). In contrast, Lc-excess values increased, and their variability decreased, when moving from the shallower to the deeper soil layers. The differences of $\delta^{18}O$ and Lc-excess between the two treatments were on average larger in the upper soil and progressively decreased when moving at depth (Fig. 6b). Xylem water samples belonging to different treatments had a comparable range of $\delta^{18}O$ and Lc-excess (Figure6b).

$\delta^{18}O$ in precipitation, throughfall, stemflow, soil, and xylem water had a sharp seasonality, with lower values during early (May) and late

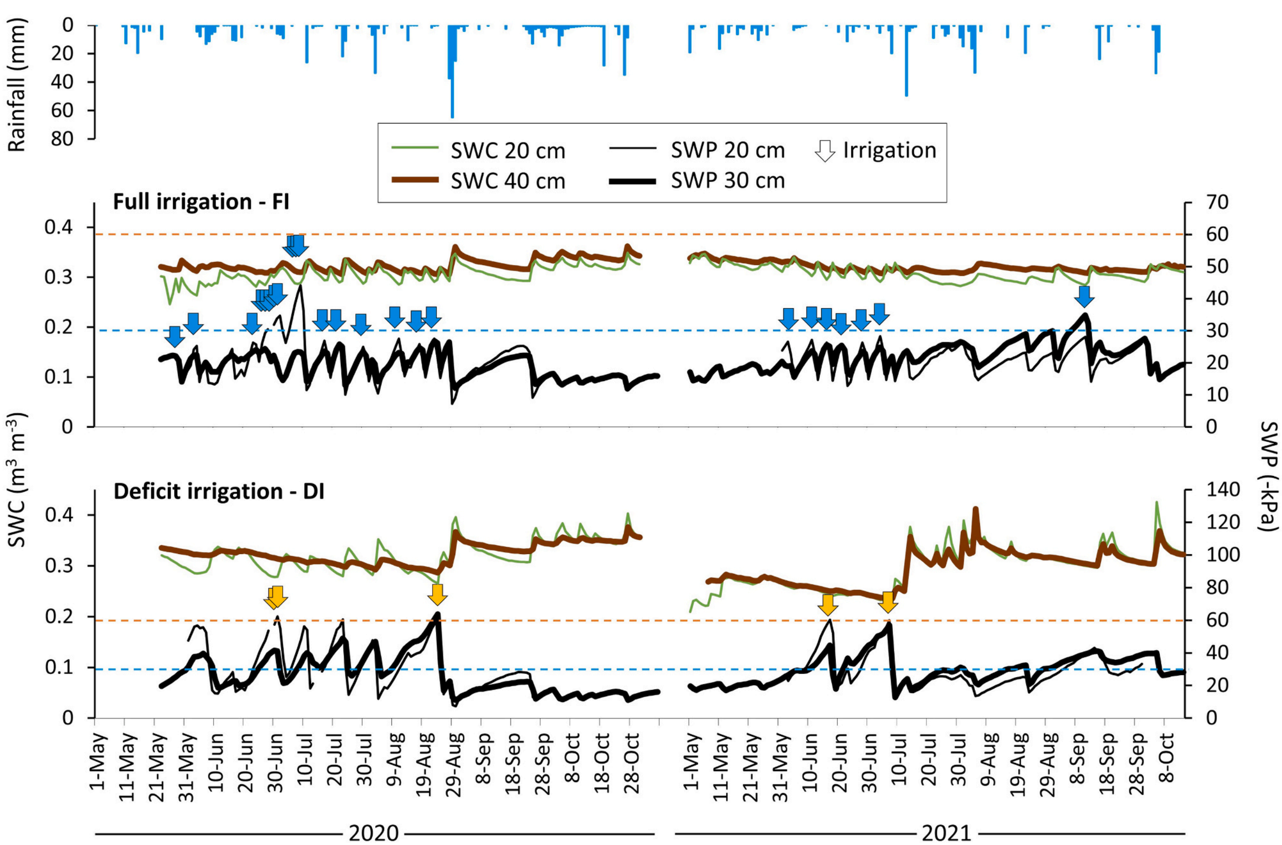

Fig. 3. Daily rainfall (top), soil water content (SWC) at 20 and 40 cm, and soil water potential (SWP) at 20 and 30 cm at FI (centre) and DI (bottom) during May/October 2020 and 2021. Arrows represent days when irrigation events occurred at FI (light blue) and DI (orange). Coloured dashed lines represent the SWP threshold of irrigation trigger at FI (light blue) and DI (orange). NOTE: During the period 25th of June - 10th of July 2020, there was a partial clogging of irrigation filters. Before the maintenance intervention, 7 irrigation events at FI and 2 events at DI supplied water at a low rate (0.6 L hr^{-1}) instead of 2.3 L hr^{-1}.

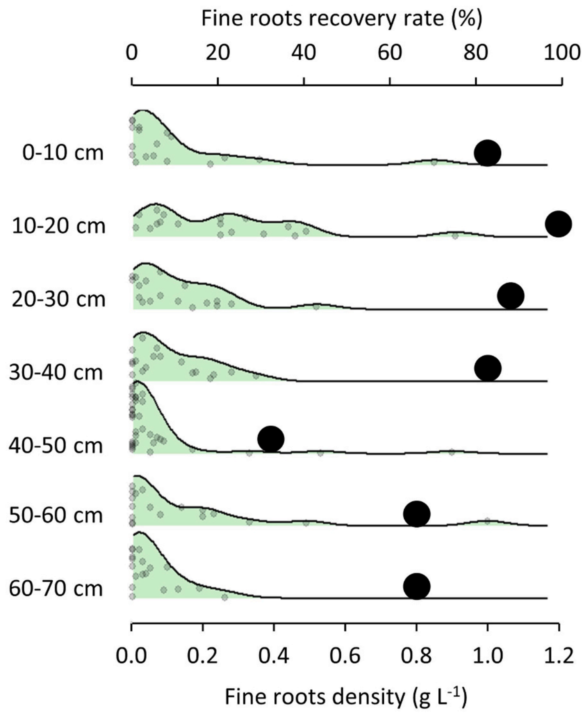

Fig. 4. Density (ridgelines) and recovery rate (dots) of fine roots at different soil depth intervals before the irrigation experiment (2018).

(October) growing season, and peaking during June/July (Fig. 7). During each sampling date, deeper soil water samples generally had lower $\delta^{18}O$ values when compared with those from the shallow soil, and xylem water samples had intermediate values among those from different soil water depths (Fig. 7).

3.4. Isotopic differences between irrigation treatments

The isotopic offset (δISO) had contrasting patterns within the soil in periods of irrigation and non-irrigation (Fig. 8). During the irrigation period, δISO was generally negative in the shallow layers, and it increased moving at depth, reaching generally positive values at 60–65 cm depth (Fig. 8a). This trend from negative to positive values was more evident during 2020. During non-irrigation periods, differences among depth intervals were less pronounced than during the irrigation period, except for the interval 60–65 cm where δISO was consistently negative during 2020 and consistently positive during 2021. Differences of δISO were not significant among xylem waters during different combinations of years and periods (Fig. 8b).

During the irrigation period, the distance in days from the latest irrigation event at the two treatments was positively related to the absolute values of δISO in xylem water ($\rho = 0.81$, $p < 0.001$; Supplementary 3). The same correlation was weak in the soil at 5–10 cm ($\rho = 0.53$, $p = 0.04$), and not significant at the other depth intervals during the same period, and for all xylem waters and soil depth intervals during the non-irrigation period of both years.

3.5. Groundwater contribution and depths of root water uptake

Based on EEMMA analysis, the groundwater fraction (F_{gw}) had a large variability at different soil depths and in xylem water during the irrigation period (Fig. 9a). This component was minor ($F_{gw} = 0.01–0.37$) in water from shallow soil (5–10 cm), it increased towards deeper soil intervals, and it was largest ($F_{gw} = 0.69–0.98$) in the deeper soil (60–65 cm). The difference between shallow and deeper soil water was more evident in DI, where the shallow depth intervals (5–10 and 10–15 cm) had lower F_{gw} than at DI, and it decreased towards the deeper soil. In contrast, xylem water had comparable F_{gw} (0.49–0.72) in the two treatments (Fig. 9a). The analyses generally performed better i) without accounting for an unknown end-member, and ii) without considering the memory effect. We did not find significant unsampled water sources, even though an unsampled end-member compatible with winter precipitation was highlighted for the 60–65 cm soil water (Supplementary 4). A significant memory effect was found in soil and xylem water at both treatments and its significance increased with soil depth (Table 2).

The average depth of root water uptake (Z_{rwu}), calculated based on the graphical/mathematical method, differed based on period, year, and treatment (Fig. 9b). During the irrigation period, Z_{rwu} was deeper at DI ($Z_{rwu} = 32.0 \pm 11.9$) than at FI ($Z_{rwu} = 19.3 \pm 14.5$). Differences between the two treatments were significant ($p < 0.001$) only during the irrigation period 2020, and were not significant during 2021 (Fig. 9b). During the period of non-irrigation, the two treatments had a comparable Z_{rwu}, even though this had a larger variability at DI ($Z_{rwu} = 29.0 \pm 16.8$) than at FI ($Z_{rwu} = 21.0 \pm 13.1$), particularly during 2020 (Fig. 9b). Within the same treatment, Z_{rwu} did not significantly differ between the two years, neither in the irrigation nor the non-irrigation periods.

IsoSource revealed a variable use of different soil intervals for root water uptake (Fig. 9c). During the non-irrigation period in both years, there was a comparable use of different soil depth intervals (F_{sd}) in DI and FI, with a larger and similar contribution from the 60–65 cm ($F_{sd} = 0.40 \pm 0.29$) and the 5–10 cm ($F_{sd} = 0.24 \pm 0.25$) depth intervals than for the 10–15 cm ($F_{sd} = 0.18 \pm 0.12$) and 20–25 cm ($F_{sd} = 0.17 \pm 0.11$) ones. During the irrigation period, the water contribution from the shallower soil depth interval (5–10 cm) was generally larger at FI (0.27 $\pm$ 0.26) than at DI (0.13 $\pm$ 0.06). This difference was significant ($p < 0.001$) only during 2020. The water contribution from the other depth intervals was not significantly different in the two treatments during the same period in both years. The variability of water contribution from different soil depth intervals was larger during 2020 than 2021 (Fig. 9c). Uncertainties of the models for single points were in the range of $F_{sd} = 0.08–0.18$.

During the irrigation period, 20 cm SWP at FI was significantly correlated with the water contribution from 5 to 10 cm ($\rho = -0.65$, $p < 0.001$), and 60–65 cm ($\rho = 0.67$, $p < 0.001$) depth intervals (Supplementary 5). Correlation between SWP and depth interval contribution was absent at DI. Similarly, SWP was strongly correlated with Z_{rwu} ($\rho = 0.67$, $p < 0.001$) during the irrigation period at FI (Supplementary 5), whereas the same correlation was absent at DI.

4. Discussion

4.1. Deficit irrigation did not cause water stress in apple trees

During the two years of investigations, the two treatments received a distinct amount of irrigation water with different frequency. DI trees had to face lower SWP and SWC than FI ones during the irrigation periods, and less water at DI was available for root uptake at 20–40 cm (where sensors were placed). Nonetheless, sap flux densities did not differ at the two treatments during the core growing season, suggesting trees from both treatments did not suffer from any physiological stress related to water deficit (cf. Zanotelli et al., 2022). Indeed, differently from other works on apple trees (e.g., Muchena et al., 2020), our aim was not to induce water stress in DI trees but, instead, to reduce water supply while ensuring the physiological demands of these trees. In our study, the difference in irrigation scheduling between the two years was not related to the rainfall amount but, instead, to the occurrence of intense rain events (> 40 mm day^{-1}). These events increased the SWC and decreased the SWP, hence cancelling the SWC/SWP differences between treatments. Intense rain events occurred early during summer 2021 when, coupled with relatively low air temperatures occurring during July and August, they delayed the additional triggering of irrigation to

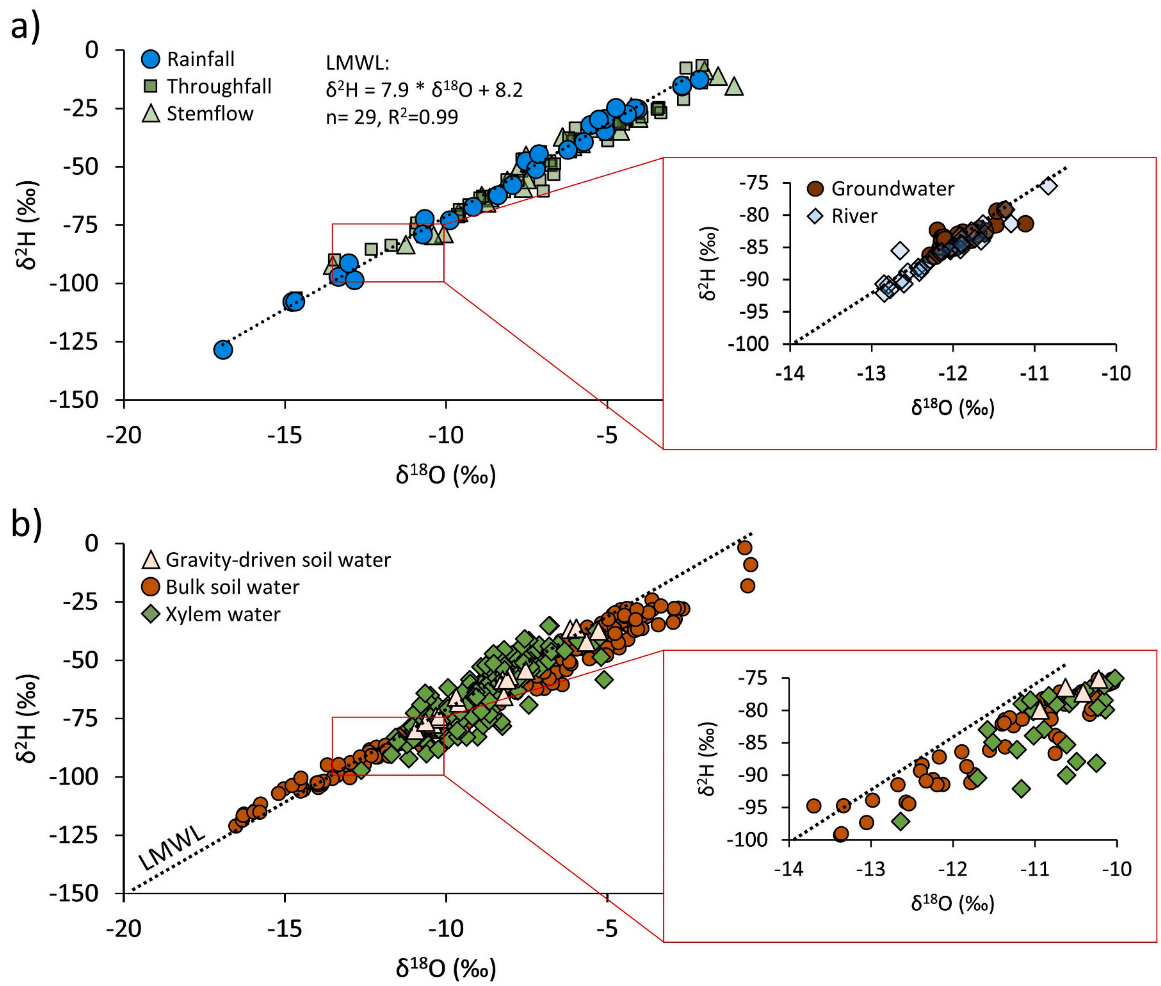

Fig. 5. Dual isotope plots showing: a) distribution of precipitation water along the local meteoric water line (LMWL), and of throughfall, stemflow, groundwater, and river water samples (close-up box for the latter two), and b) distribution of gravity-driven (obtained with suction cups) and bulk (obtained with cryogenic vacuum distillation) soil water, and xylem water samples, with the LMWL and the close-up maintained as reference.

early September.

4.2. Isotopic conditions of the ecohydrological system

The isotopic signatures of the upper and intermediate soil water and xylem water were strongly driven by the seasonality of precipitation, with overall rising $\delta^{18}O$ values during summer and declining values during autumn. This is typical of temperate climates with alternance of warm and cold seasons (Araguas-Araguas et al., 2000; Sprenger et al., 2016; Allen et al., 2019). The patterns of $\delta^{18}O$ in soil water generally agree with those of precipitation, but are modified by: i) the rainfall interception by the canopy, causing slight differences between precipitation and throughfall and stemflow water (see also Penna et al., 2021); ii) the evaporative fractionation occurring in the topsoil, with associated transfer of isotopically enriched water to the deeper soil via subsequent mixing or translatory flow imparted by rain events (Sprenger et al., 2016); iii) the supply of anti-frost sprinkler irrigation during springtime and drip irrigation (groundwater) during summer, being both water types more depleted in heavy isotopes than the rainfall occurring in the same periods. Water from the deeper soil (60–65 cm) was generally the least responsive to the isotopic seasonality imparted to the soil system by precipitation. During early summer, this deep layer had very depleted isotopic values, in the range of those of winter precipitation ($\delta^{18}O$ in the range of −17/-14‰ during January/February; not shown because collected during 2022). During 2020, $\delta^{18}O$ values of the deep soil water increased starting from the onset of irrigation at FI, and after the occurrence of intense rain events at DI. These events were the same responsible for the sudden rise of SWP and SWC discussed in the previous paragraph. Afterwards, also deep soil water aligned on the seasonal isotopic behaviour of the system. During 2021, the deep soil water had an earlier rise of $\delta^{18}O$ values at both treatments, likely because of an anticipated occurrence of relatively intense rain events.

Xylem water was more evidently aligned with the isotopic seasonality of precipitation during the growing season. This testifies a smoothened response of this water pool to short-term variations, when compared with that of the soil.

4.3. Isotopic differences between treatments are more evident for soil than for trees

The differences in $\delta^{18}O$ between irrigation treatments, calculated for single sampling dates as isotopic offset - δISO, were particularly evident for water in the shallow and intermediate depth intervals (i.e., 5–30 cm) and during the irrigation periods. We attribute the consistently more depleted isotopic values at FI than at DI to a higher amount of irrigation water (more depleted in heavy isotopes than rainwater) applied to FI. The volumes of irrigation supply were 5.7-fold higher at FI than at DI during 2020, and only 2.3-fold higher during 2021. Thus, not surprisingly, the isotopic offset in the shallow and intermediate soil water was on average more negative during 2020 (Supplementary 6). As expected, the isotopic offset tended to be less pronounced when moving deeper into the soil, because of the reduced infiltration of irrigation water with

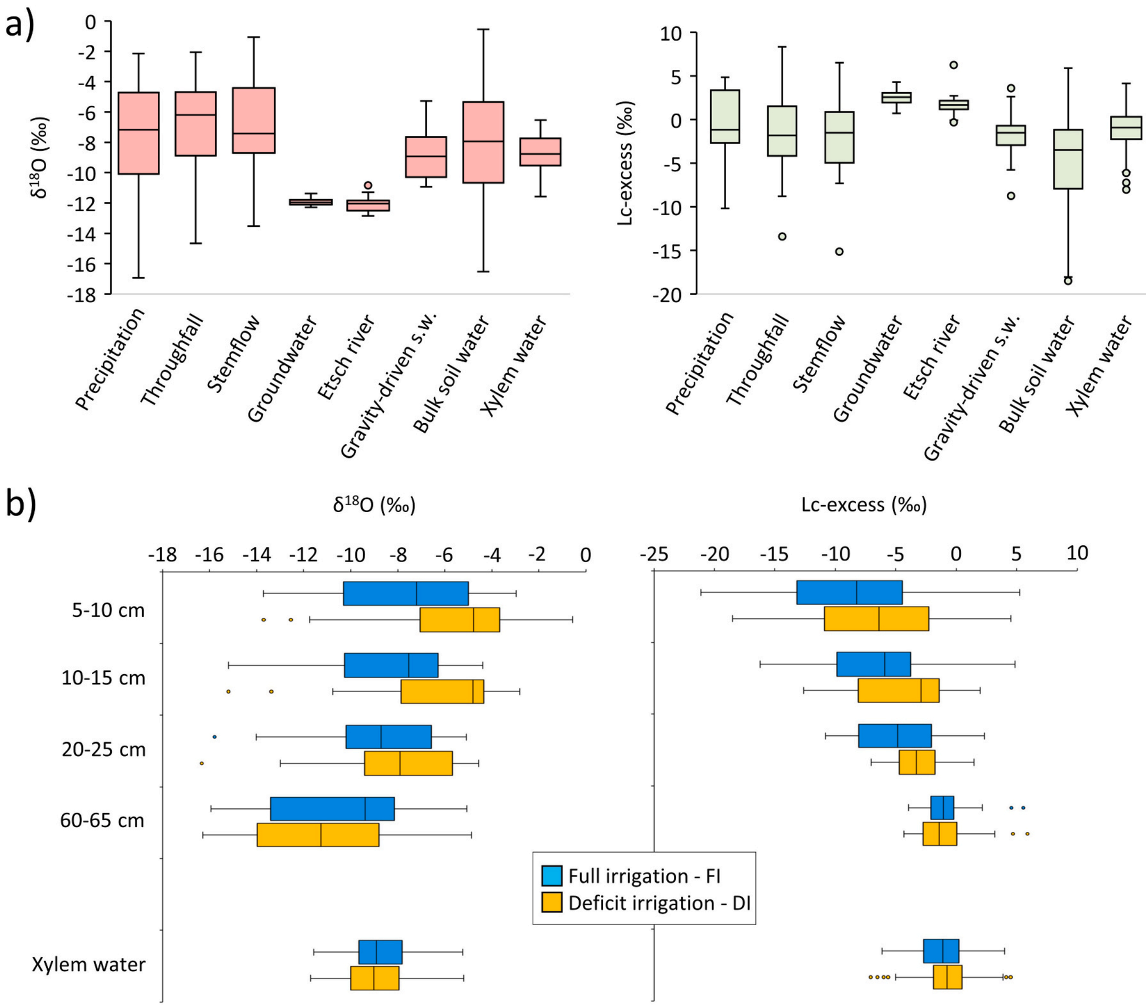

Fig. 6. Boxplots of $\delta^{18}O$ and Lc-excess (‰) for (a) different water pools, and (b) for bulk soil water at different depths and xylem water, categorised per irrigation treatment.

depth. Interestingly, during the irrigation period, the isotopic offset had a reversal behaviour at the deeper soil interval (60–65 cm), with generally positive values (DI more depleted in heavy isotopes than FI). This can be explained by the very negative isotopic values found at this depth interval (see Section 4.2) in the earlier part of this period. The rain events causing $\delta^{18}O$ rise of the deep soil water occurred later during 2020 (late August) than during 2021 (early July). While these events influenced the isotopic behaviour of the deeper soil at DI, the rise of $\delta^{18}O$ occurred one month earlier at FI during 2020. This was likely made possible by the infiltration of water from several irrigation events, providing isotopically less negative water when compared with that of the winter precipitation. The isotopic enrichment provided by this water might be also caused by translatory effects and/or mixing with (less negative) rainwater already stored within the soil (Sprenger et al., 2016). For the same reason, water from the deeper soil was consistently more depleted in heavy isotopes at DI during the irrigation period 2020 but not during that of 2021, when the total number of irrigation events was lower.

In contrast with what was found for soil water, the isotopic offset of xylem water was generally low or absent during both years and periods. This might be related to a strong dampening of the isotopic signal in xylem water. This isotopic smoothening was demonstrated in the same field by Giuliani et al. (2023), who applied deuterated water by simulating drip irrigation. The authors tracked the movements of deuterated water within the soil, accounting for up to 100% of the bulk water composition close to the dripper and in the shallow soil (0–20 cm). By contrast, the fraction of irrigated water never exceeded 4–5% of the total xylem water present in the shoots until the end of the experiment (32 hours; Giuliani et al., 2023). Comparable findings were reported for an apple orchard in the same area, where the calculated fraction of deuterated water never exceeded 8% of the total xylem water in 168 hours from the irrigation supply (Aguzzoni et al., 2022). These low percentages of irrigation against pre-irrigation water were attributed to a combination of: i) a prevalent use of deeper soil water, that was not or poorly reached by irrigation during the experiments; ii) a slow or inefficient mixing of the deuterated water with that already present in the xylem tissues (Aguzzoni et al., 2022); and/or iii) the extraction of a considerable amount of intracellular xylem water with the cryogenic vacuum distillation technique (Giuliani et al., 2023). Notably, we applied the same water extraction method, which causes isotopic fractionation especially for $\delta^{2}H$ and thus modifies the isotopic signature of the water extracted from the plant tissues (Chen et al., 2020; Wen et al., 2022). Even if we used $\delta^{18}O$ as tracer, the biases introduced with this technique cannot be excluded (Millar et al., 2022). Despite the smoothened isotopic offset in xylem water, we found a strong correlation between the difference in days elapsed from the latest irrigation supply and the isotopic offset. This suggests that different irrigation scheduling does influence xylem water isotopic conditions. In general, a relatively rapid isotopic response of apple trees to water supply was demonstrated by Giuliani et al. (2023), who detected the first arrival of deuterated water in xylem tissues already after 4–6 hours from irrigation.

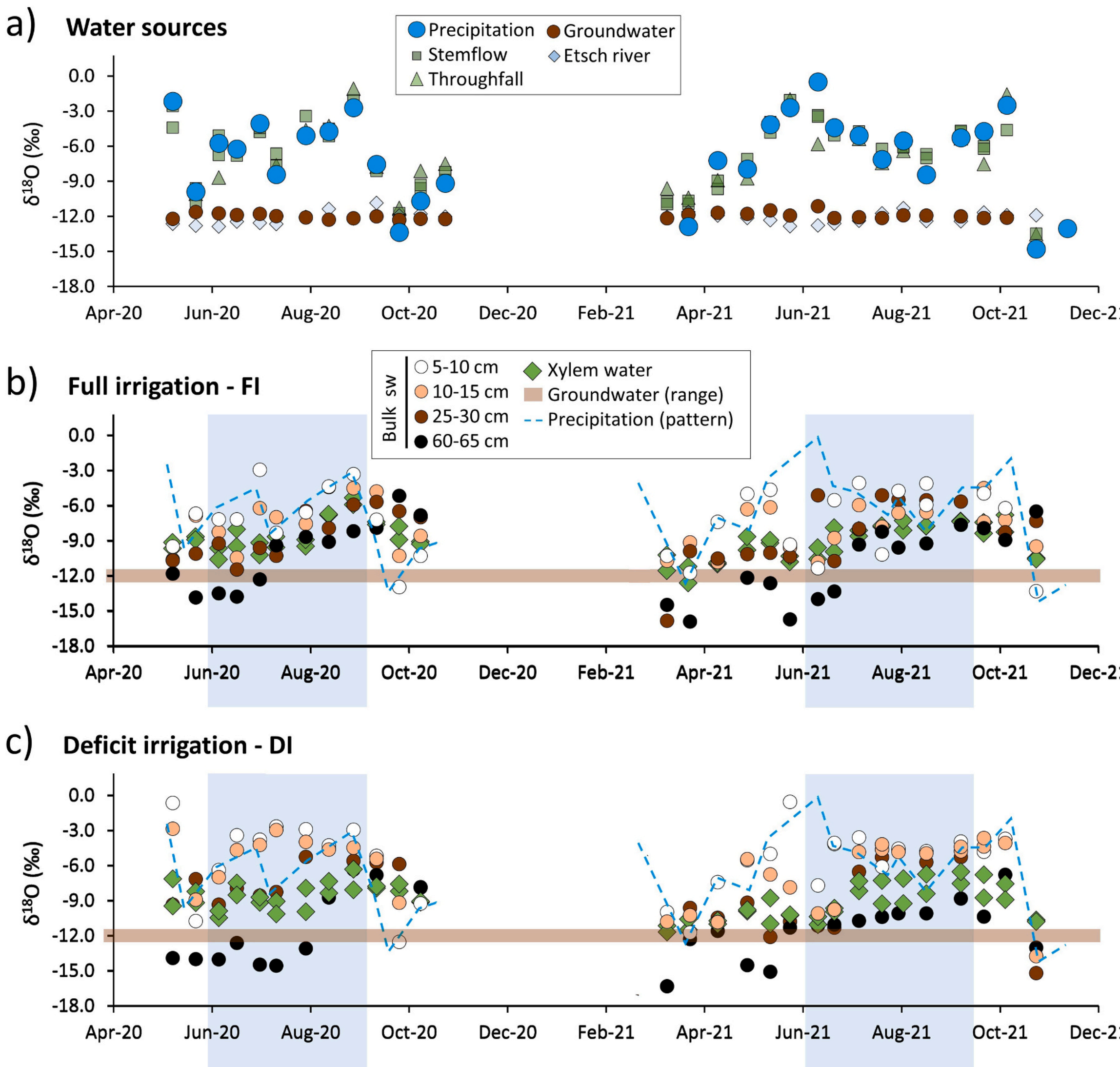

Fig. 7. Time series of $\delta^{18}O$ (‰) in a) Hydrological resources, and in the soil at different depth intervals and xylem water samples belonging to b) Full irrigation and c) Deficit irrigation treatments. For the latter two, the series of precipitation (dashed line) and the range of groundwater (band) are shown as reference. The pale blue backgrounds represent the irrigation periods.

During the periods of non-irrigation, the isotopic differences between treatments were strongly smoothened when compared with the irrigation periods, even though slight differences persisted within the soil. This may testify a long-term response of soil water to shifting contributions from different resources. The consistently negative isotopic offset during the non-irrigation period 2020 (September-October) may have resulted from translatory flows imparted by the intense rain event of late August, moving a negative isotopic offset of the shallow/intermediate soil (occurring during the irrigation period) to the deeper soil. Accordingly, rain events that occurred during the non-irrigation period 2021 were not intense enough to establish efficient translatory mechanisms, and the two treatments may have maintained their isotopic differences in this layer. In general, our first hypothesis on the isotopic differences between DI and FI treatments can be retained. However, the magnitude and timing of these differences result from a combination of direct (irrigation supply, intense rain events) and indirect (translatory flows, water infiltration) effects favouring reversed response in the deeper soil, and a smoothened isotopic offset in xylem water.

4.4. Irrigation supply increases the groundwater fraction in the shallow soil

The groundwater fraction, estimated with EEMMA, differed in the two treatments only within the shallow soil, where it was larger at FI than at DI, as expected by a larger amount of irrigation supplied to FI. However, our second hypothesis can only be partially accepted, since no evident differences between the two treatments were found in the deeper soil and in xylem water. The natural isotopic gradient occurring within the soil profile, observed in natural systems (Sprenger et al., 2016) as well as in crops (Cao et al., 2018; Penna et al., 2021) with increasingly negative values of $\delta^{18}O$, was the main responsible of the increasing groundwater fraction with depth. The two irrigation treatments had sharply different groundwater fractions in the upper and intermediate soil (5–25 cm). This was particularly evident at 5–10 cm, where this component was in the order of 30–50% at FI, and negligible (0–5%) at DI. This is compatible with a 3–5-fold larger frequency of irrigation supplied at FI than at DI.

Notably, we found significant memory effects in soil and xylem water, again indicating slow isotopic responses to ecohydrological seasonality. An unsampled end-member, compatible with winter

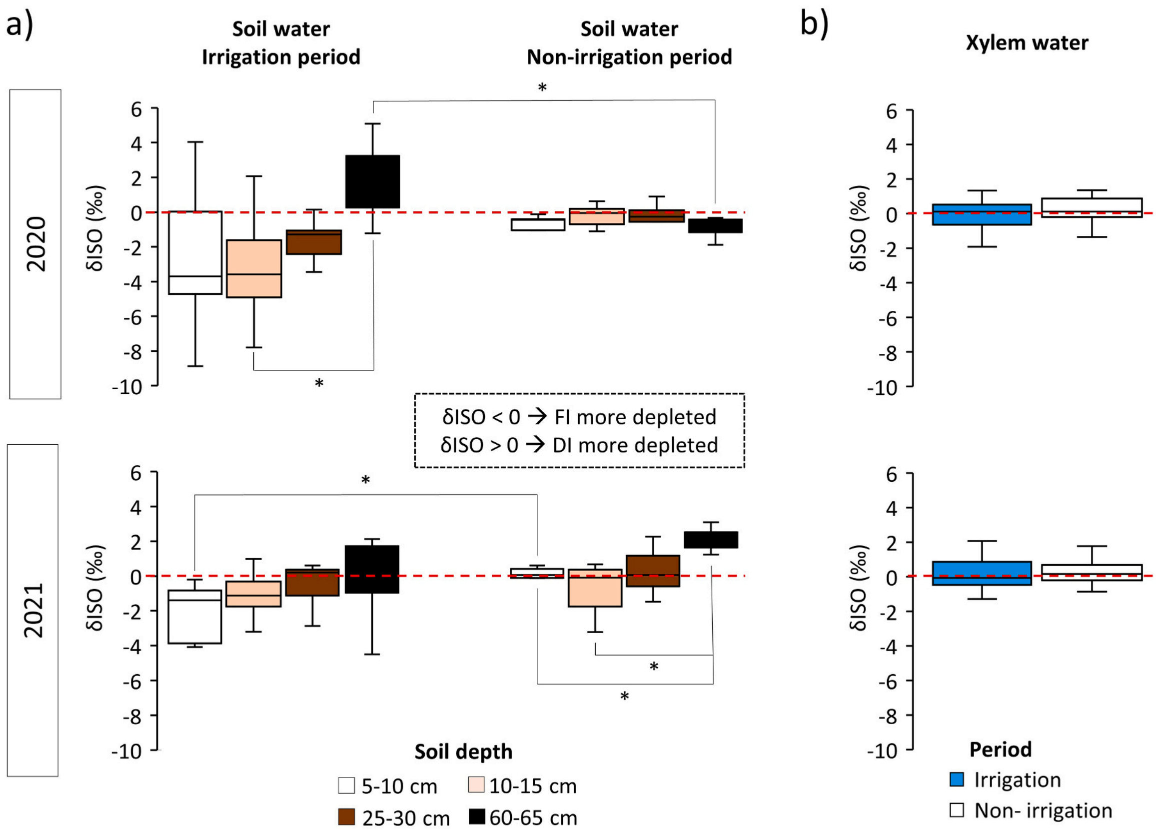

Fig. 8. Boxplots of δISO (‰) at a) soil water at different depths and b) xylem water in the two treatments during the irrigation and non-irrigation periods 2020 and 2021. Significant pairwise comparisons (Kruskal-Wallis test) are highlighted with asterisks (*$p < 0.05$).

precipitation (Supplementary 4) was surprisingly not considered as significant by EEMMA within the soil at 60–65 cm, but this is likely due to the necessary pooling of several mixture values, most of which were in the range of their potential end-members. The little amount of data points in the series, and consequent necessity for data aggregation based on DOY, might have also hindered the modelling of a significant memory effect at 60–65 cm in DI.

4.5. Deficit irrigation enhances the root water uptake from the deeper soil

Deficit irrigation aims at reducing the amount of irrigation water without causing severe stress to apple trees. In Binnenland, Ben Abdelkader et al. (2022) found comparable apple production in FI (93 ± 12 t ha^{-1}) and DI (95 ± 12 t ha^{-1}) treatments during the 2020 harvest. In the present experiment, SWP of FI trees ranged from 0 to −30 kPa, while DI trees experienced some periods when water was slightly less available, still never below −60 kPa. However, it should be considered that such values of SWP were measured in the volume of soil mostly affected by the irrigation system. Leaf transpiration of potted apple trees of the same variety used in the present experiment was unaffected by soil water availability until midday stem water potential was −1.45 MPa and soil water potential was −0.45 MPa (Ben Abdelkader et al., 2022). Since apple trees did not experience physiological stress during the period of investigation, not surprisingly we found a contrasting use of water from different depths in the two irrigation treatments (Cao et al., 2018). Indeed, both graphical/mathematical estimation and mixing models converged to a higher use of deeper soil water in DI than in FI plants. This was particularly evident during the irrigation period 2020, when the average depth of root water uptake at DI was on average 2-fold deeper than at FI. Also mixing models revealed a roughly 2-fold lower contribution from the shallow soil (5–10 cm), counterbalanced by a larger contribution from the intermediate (20–25 cm) and deeper (60–65 cm) soil water. The correlation between SWP and the contribution from shallowest and deepest soil water, and between SWP and the average depth of root water uptake, was only evident at FI. This suggests that DI plants physiologically shaped their water use to the reduced water availability. FI plants adapted their root uptake to the short-term variations of water availability in the shallow soil, as also testified by large standard deviation of the 5–10 cm contribution to xylem water during the irrigation period. In contrast, DI plants more often used deeper resources as “safe harbour” from water shortages often occurring in the shallow soil. This long-term modification would also explain why the depth of root water uptake, and the use of deeper soil water, were slightly larger at DI than at FI even during the periods of non-irrigation.

In general, the depth interval at which the density and recovery rate of fine roots were highest matched the overall range of root water uptake depth during all periods and years (10–40 cm), in line with what was found by another study in an apple orchard close to our study site (Penna et al., 2021). While we estimated the fine roots distribution only before the trial, all the isotopically investigated depths could be potentially accessed by fine roots in our study, leaving room for apple trees to adapt their water uptake based on the availability of water at different depths. Like other plants, apple trees can adapt their fine root distribution based on the shifting availability of water. For example, in an experimental apple orchard (cv. Gloster on M26 rootstock) in Poland, a larger density of fine roots was found in the shallow soil of fully irrigated treatments, and in the deeper soil in non-irrigated treatments after 12 years of differentiated treatment (Sokalska et al., 2009). Similarly, under arid conditions of northern China, the fine root distribution in the shallow soil was positively related to the frequency of irrigation supplied during two years to the apple plants (Du et al., 2018). However, the response of fine roots development to different irrigation supply can be complex, and depends on the year of trial and seasonality (Svoboda et al., 2023), or to the different types of irrigation (e.g., drip versus surface irrigation)

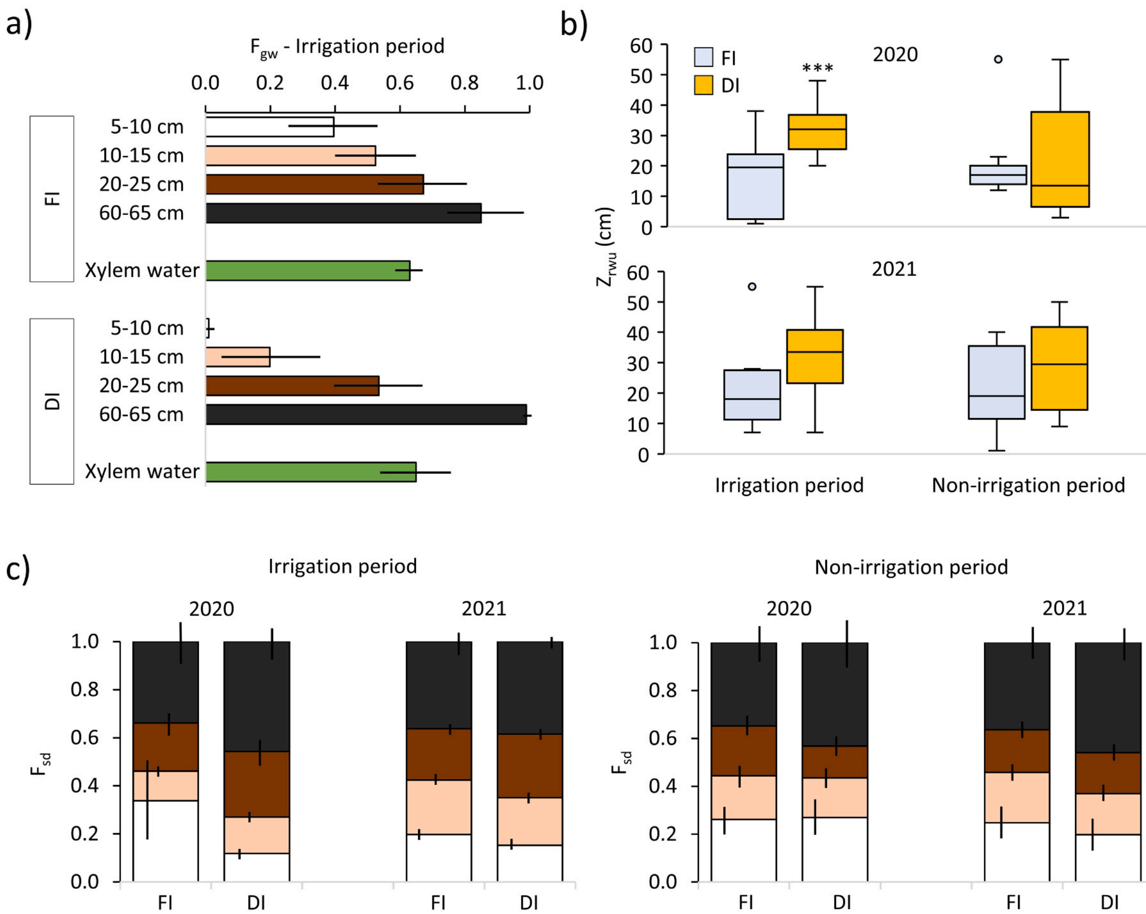

Fig. 9. a) Groundwater fraction - F_{gw} (against rainwater fraction) at different soil depth intervals and xylem water at FI and DI during the irrigation period, resulting from EEMMA; b) Average depth of root water uptake (Z_{rwu}) at FI and DI during the irrigation and non-irrigation periods of 2020 and 2021; c) Summary bar plots of the contribution to xylem water fluxes from different soil depth intervals (F_{sd}). Black bars represent half of standard deviation.

Table 2
Estimation of memory effect in EEMMA. For each mixture, we provide the p-values at the two irrigation treatments. $^{*}p \leq 0.05$, $^{**}p \leq 0.01$, $^{***}p \leq 0.001$, $^{ns}p > 0.05$.

	FI	DI
Soil water 5–10 cm	1.8*	3.4**
Soil water 10–15 cm	2.7*	4.0**
Soil water 20–25 cm	2.8**	3.5**
Soil water 60–65 cm	0.4 ns	0.3 ns
Xylem water	2.4**- 4.9***	2.0**- 4.2***

that are compared (Li et al., 2019). Of course, these vertical compensations of root water uptake can only occur as long as enough water is available for plants in some part of the soil profile accessed by fine roots.

5. Conclusions

We found that the plasticity in root water uptake from different soil depths allowed apple trees to meet transpirative demands under a deficit irrigation of moderate intensity. The different water supply in the full and deficit irrigation caused different isotopic signatures in the soil. The same differences were not evident in xylem water. The similar isotopic signature in xylem water of the two treatments was caused by a combination of different isotopic fingerprints in the soil profile and a contrasting uptake of water from different depths by apple trees. Indeed, plants belonging to the deficit irrigation treatment used more water from the deeper soil and less water from the shallow soil, when compared to plants subject to full irrigation. These outcomes offer an isotope-based explanation of the comparable sap fluxes and fruit yields in the two treatments, and endorse a process-oriented management of precision irrigation. Understanding how much our results can be extended to other crops, soil conditions, and climates would be relevant to inform sustainable water management in agriculture.

CRediT authorship contribution statement

Daniele Penna: Writing – review & editing, Funding acquisition. **Damiano Zanotelli:** Writing – review & editing, Validation, Supervision, Methodology, Investigation, Formal analysis, Data curation, Conceptualization. **Francesco Comiti:** Writing – review & editing, Supervision, Project administration, Methodology, Funding acquisition, Conceptualization. **Agnese Aguzzoni:** Writing – review & editing, Investigation. **Nicola Giuliani:** Writing – review & editing. **Ahmed Ben Abdelkader:** Writing – review & editing, Investigation, Data curation. **Stefano Brighenti:** Writing – original draft, Validation, Software, Methodology, Investigation, Formal analysis, Data curation, Conceptualization. **Massimo Tagliavini:** Writing – review & editing, Supervision, Project administration, Methodology, Conceptualization.

Declaration of Competing Interest

The authors declare that they have no known competing financial interests or personal relationships that could have appeared to influence the work reported in the paper.

Data Availability

Data will be made available on request.

Acknowledgments

We thank Christian Ceccon for his support in the laboratory and for the IRMS analyses. This research was supported by the PRIN MIUR 2017SL7ABC_005 WATZON (Water mixing in the critical zone) Project and by the MIUR – Dipartimento di Eccellenza DIST department funds. We thank Luca Maraldo and the Hydrological of the Autonomous Province of Bolzano/Bozen for delivering the meteorological data of the automatic weather station of Auer/Ora.

Appendix A. Supporting information

Supplementary data associated with this article can be found in the online version at doi:10.1016/j.agwat.2024.108870.

References

Aguzzoni, A., Engel, M., Zanotelli, D., Penna, D., Comiti, F., Tagliavini, M., 2022. Water uptake dynamics in apple trees assessed by an isotope labelling approach. Agric. Water Manag. *266* https://doi.org/10.1016/j.agwat.2022.107572.

Allen, S.T., Kirchner, J.W., Braun, S., Siegwolf, R.T.W., Goldsmith, G.R., 2019. Seasonal origins of soil water used by trees. Hydrol. Earth Syst. Sci. *23*, 1199–1210. https://doi.org/10.5194/hess-23-1199-2019.

Araguas-Araguas, L., Froehlich, K., Rozanski, K., 2000. Deuterium and oxygen-18 isotope composition of precipitation and atmospheric moisture. Hydrol. Process. 14 (8), 1341–1355. https://doi.org/10.1002/1099-1085(20000615)14:8%3C1341::AID-HYP983%3E3.0.CO;2-Z.

Autonomous Province of Bozen/Bolzano [APB], 2023. Meteorological series of the period 1983-2022, Auer/Ora. Retrieved from ⟨www.meteo.provincia.bz.it⟩.

Ben Abdelkader, A., Thalheimer, M., Petrillo, M., Tagliavini, M., Zanotelli, D., 2022. Automatic irrigation scheduling based on soil water potential thresholds allows water savings in a highly productive apple orchard. Acta Hortic., 2022 563–570. https://doi.org/10.17660/ActaHortic.2022.1346.71.

Beyer, M., Penna, D., 2021. On the spatio-temporal under-representation of isotopic data in ecohydrological studies. Front. Water 3, 643013. https://doi.org/10.3389/frwa.2021.643013.

Brooks, P.D., Chorover, J., Fan, Y., Godsey, S.E., Maxwell, R.M., McNamara, J.P., Tague, C., 2015. Hydrological partitioning in the critical zone: Recent advances and opportunities for developing transferable understanding of water cycle dynamics. Water Resour. Res. *51*, 6973–6987. https://doi.org/10.1002/2015WR017039.

Canet-Martí, A., Morales-Santos, A., Nolz, R., Langergraber, G., Stumpp, C., 2023. Quantification of water fluxes and soil water balance in agricultural fields under different tillage and irrigation systems using water stable isotopes. Soil Tillage Res. *231*, 105732 https://doi.org/10.1016/j.still.2023.105732.

Cao, X., Yang, P., Engel, B.A., Li, P., 2018. The effects of rainfall and irrigation on cherry root water uptake under drip irrigation. Agric. Water Manag. *197*, 9–18. https://doi.org/10.1016/j.agwat.2017.10.021.

Chen, Y., Helliker, B.R., Tang, X., Li, F., Zhou, Y., Song, X., 2020. Stem water cryogenic extraction biases estimation in deuterium isotope composition of plant source water. Proc. Natl. Acad. Sci. USA *117* (52), 33345–33350. https://doi.org/10.1073/pnas.2014422117.

Cui, J., Tian, L., Gerlein-Safdi, C., Qu, D., 2017. The influence of memory, sample size effects, and filter paper material on online laser-based plant and soil water isotope measurements. Rapid Commun. Mass Spectrom. *31*, 509–522. ⟨https://doidoi.org/10.1002/rcm.7824⟩.

Dansgaard, W., 1964. Stable isotopes in precipitation. Tellus *16* (4), 436–468. https://doi.org/10.1111/j.2153-3490.1964.tb00181.x.

Du, S., Tong, L., Kang, S., Li, F., Du, T., Li, S., Ding, R., 2018. Alternate partial root-zone irrigation with high irrigation frequency improves root growth and reduces unproductive water loss by apple trees in arid north-west China. Front. Agric. Sci. Eng. *5*, 188–196. https://doi.org/10.15302/J-FASE-2017176.

FAO (2020). The State of Food and Agriculture 2020. Overcoming water challenges in agriculture. FAO, Rome. 220 pp. Available at: ⟨https://doi.org/10.4060/cb1447en⟩.

Frasier, I., Noellemeyer, E., Fernández, R., Quiroga, A., 2016. Direct field method for root biomass quantification in agroecosystems. MethodsX *3*, 513–519. https://doi.org/10.1016/j.mex.2016.08.002.

Giuliani, N., Aguzzoni, A., Penna, D., Tagliavini, M., 2023. Estimating uptake and internal transport dynamics of irrigation water in apple trees using deuterium-enriched water. Agric. Water Manag. *289*, 108532 https://doi.org/10.1016/j.agwat.2023.108532.

Goebel, T.S., Lascano, R.J., 2019. Rainwater use by cotton under subsurface drip and center pivot irrigation. Agric. Water Manag. *215*, 1–7. https://doi.org/10.1016/j.agwat.2018.12.027.

Gröning, M., Lutz, H.O., Roller-Lutz, Z., Kralik, M., Gourcy, L., Pöltenstein, L., 2012. A simple rain collector preventing water reevaporation dedicated for $\delta^{18}O$ and $\delta^{2}H$ analysis of cumulative precipitation samples. J. Hydrol. 448–449, 195–200. https://doi.org/10.1016/j.jhydrol.2012.04.041.

IBM (2018). SPSS Statistics software, v.27.

Kirchner, J.W., 2023. Mixing models with multiple, overlapping, or incomplete end-members, quantified using time series of a single tracer. Geophys. Res. Lett. *50*, e2023GL104147 https://doi.org/10.1029/2023GL104147.

Kirchner, J.W., Benettin, B., van Meerveld, I., 2023. Instructive Surprises in the Hydrological Functioning of Landscapes. Annu. Rev. Earth Planet. Sci. *51* (1), 277–299. https://doi.org/10.1146/annurev-earth-071822-100356.

Koeniger, P., Marshall, J.D., Link, T., Mulch, A., 2011. An inexpensive, fast, and reliable method for vacuum extraction of soil and plant water for stable isotope analyses by mass spectrometry. Rapid Commun. Mass Spectrom. 25 (20), 3041–3048. https://doi.org/10.1002/rcm.5198.

Landgraf, J., Tetzlaff, D., Dubbert, M., Dubbert, D., Smith, A., Soulsby, C., 2022. Xylem water in riparian willow trees (*Salix alba*) reveals shallow sources of root water uptake by in situ monitoring of stable water isotopes. Hydrol. Earth Syst. Sci. *26*, 2073–2092. https://doi.org/10.5194/hess-26-2073-2022.

Landwehr, J.M., and Coplen, T.B. (2006). Line-conditioned excess: A new method for characterizing stable hydrogen and oxygen isotope ratios in hydrologic systems (IAEA-CSP–26/P). International Atomic Energy Agency (IAEA).

Lauteri, M., Alessio, G.A., Paris, P., 2005. Using oxygen stable isotopes to investigate the soil-plant-atmosphere hydraulic continuum in complex stands of walnut. Acta Hortic. (705), 223–230. https://doi.org/10.17660/ActaHortic.2005.705.27.

Li, P., Tan, H., Wang, J., Cao, X., Yang, P., 2019. Evaluation of Water Uptake and Root Distribution of Cherry Trees under Different Irrigation Methods. Water *11*, 495. https://doi.org/10.3390/w11030495.

Li, H., Wang, J., Wang, C., Wang, G., Zhang, X., Cui, B., Song, B., 2024. Apple trees utilize 3–5% of root biomass in the weathered rock layer to absorb 33–34% of their transpiration water consumption. Agric., Ecosyst. Environ. *359* https://doi.org/10.1016/j.agee.2023.108743.

Liang, Z., Liu, X., Xiong, J., Xiao, J., 2020. Water Allocation and Integrative Management of Precision Irrigation: A Systematic Review. Water *12*, 3135. https://doi.org/10.3390/w12113135.

Liu, J., Si, Z., Wu, L., Chen, J., Gao, Y., Duan, A., 2021. Using stable isotopes to quantify root water uptake under a new planting pattern of high-low seed beds cultivation in winter wheat. Soil Tillage Res. *205*, 104816 https://doi.org/10.1016/j.still.2020.104816.

Liu, Y., Zhang, X., Zhao, S., Ma, H., Qi, G., Guo, S., 2019. The Depth of Water Taken up by Walnut Trees during Different Phenological Stages in an Irrigated Arid Hilly Area in the Taihang Mountains. Forests 10, 121. https://doi.org/10.3390/f10020121.

Ma, Y., Song, X., 2016. Using stable isotopes to determine seasonal variations in water uptake of summer maize under different fertilization treatments. Sci. Total Environ. *550*, 471–483. https://doi.org/10.1016/j.scitotenv.2016.01.148.

Ma, Y., Song, X., 2019. Applying stable isotopes to determine seasonal variability in evapotranspiration partitioning of winter wheat for optimizing agricultural management practices. Sci. Total Environ. *654*, 633–642. https://doi.org/10.1016/j.scitotenv.2018.11.176.

Mahindawansha, A., Orlowski, N., Kraft, P., Rothfuss, Y., Racela, H., Breuer, L., 2018. Quantification of plant water uptake by water stable isotopes in rice paddy systems. Plant Soil *429*, 281–302. https://doi.org/10.1007/s11104-018-3693-7.

Mekonnen, M.M., Hoekstra, A.Y., 2020. Sustainability of the blue water footprint of crops. Adv. Water Resour. *143* https://doi.org/10.1016/j.advwatres.2020.103679.

Millar, C., Janzen, K., Nehemy, M.F., Koehler, G., Hervé-Fernández, P., Wang, H., Orlowski, N., Barbeta, A., McDonnell, J.J., 2022. On the urgent need for standardization in isotope-based ecohydrological investigations. Hydrol. Process. *36* (10), e14698 https://doi.org/10.1002/hyp.14698.

Muchena, L., Dzikiti, S., Lötze, E., Midgley, S.J.E., 2020. Using sap flow sensors to study the influence of rootstock and mid-summer water deficit on transpiration of apple trees in South Africa. Acta Hortic. (*1300*), 201–210. https://doi.org/10.17660/ActaHortic.2020.1300.26.

Pastor, A.V., Palazzo, A., Havlik, P., Biemans, H., Wada, Y., Obersteiner, M., Kabat, P., Ludwig, F., 2019. The global nexus of food–trade–water sustaining environmental flows by 2050. Nat. Sustain. *2* (2019), 499–507. https://doi.org/10.1038/s41893-019-0287-1.

Penna, D., Geris, J., Hopp, L., Scandellari, F., 2020. Water sources for root water uptake: Using stable isotopes of hydrogen and oxygen as a research tool in agricultural and agroforestry systems. Agric., Ecosyst. Environ. *291*, 06790. https://doi.org/10.1016/j.agee.2019.106790.

Penna, D., Stenni, B., Šanda, M., Wrede, S., Bogaard, T.A., Michelini, M., Fischer, B.M.C., Gobbi, A., Mantese, N., Zuecco, G., Borga, M., Bonazza, M., Sobotková, M., Čejková, B., Wassenaar, L.I., 2012. Technical Note: Evaluation of between-sample memory effects in the analysis of δ2H and δ18O of water samples measured by laser spectroscopes. Hydrol. Earth Syst. Sci. *16*, 3925–3933. https://doi.org/10.5194/hess-16-3925-2012.

Penna, D., Zanotelli, D., Scandellari, F., Aguzzoni, A., Engel, M., Tagliavini, M., Comiti, F., 2021. Water uptake of apple trees in the Alps: Where does irrigation water go? Ecohydrology *14*. https://doi.org/10.1002/eco.2306.

Philipps, D.L., Gregg, J.W., 2003. Source partitioning using stable isotopes: coping with too many sources. Oecologia *136*, 261–269. https://doi.org/10.1007/s00442-003-1218-3.

R Core Team (2021). R: A language and environment for statistical computing. R Foundation for Statistical Computing, Vienna, Austria. URL ⟨https://www.R-project.org/⟩.

Rozanski, K., Araguás-Araguás, L., Gonfiantini, R., 1993. Isotopic patterns in modern global precipitation. In: Swart, P.K., Lohmann, K.C., Mckenzie, J., Savin, S. (Eds.), Climate change in continental isotopic records, Geophysical Monograph Series, (Vol.

78. American Geophysical Union, Washington, DC. https://doi.org/10.1029/GM078p0001.
Shi, P., Gai, H., Li, Z., 2023a. Partitioned soil water balance and its link with water uptake strategy under apple trees in the Loess-covered region. e2022WR032670 Water Resour. Res. *59*. https://doi.org/10.1029/2022WR032670.
Shi, P., Gai, H., Liu, W., Li, Z., 2023b. Links of apple tree water uptake strategies with precipitation and soil water dynamics in the deep loess deposits. J. Hydrol. *623*, 129829 https://doi.org/10.1016/j.jhydrol.2023.129829.
Siebert, S., Burke, J., Faures, J.M., Frenken, K., Hoogeveen, J., Döll, P., Portmann, F.T., 2010. Groundwater use for irrigation – a global inventory. Hydrol. Earth Syst. Sci. *14*, 1863–1880. https://doi.org/10.5194/hess-14-1863-2010.
Sokalska, D.I., Haman, D.Z., Szewczuk, A., Sobota, J., Dereń, D., 2009. Spatial root distribution of mature apple trees under drip irrigation system. Agric. Water Manag. *96*, 917–924. https://doi.org/10.1016/j.agwat.2008.12.003.
Sprenger, M., Leistert, H., Gimbel, K., Weiler, M., 2016. Illuminating hydrological processes at the soil-vegetation-atmosphere interface with water stable isotopes. Rev. Geophys. *54*, 674–704. https://doi.org/10.1002/2015RG000515.
Sun, S.J., Meng, P., Zhang, J.S., Wan, X., 2011. Variation in soil water uptake and its effect on plant water status in Juglans regia L. during dry and wet seasons. Tree Physiol. 31 (12), 1378–1389. https://doi.org/10.1093/treephys/tpr116Tom%E8.
Svoboda, P., Haberle, J., Moulik, M., Raimanová, I., Kurešová, G., Mészáros, M., 2023. The Effect of Drip Irrigation on the Length and Distribution of Apple Tree Roots. Horticulturae *9*, 405. https://doi.org/10.3390/horticulturae9030405.
Thalheimer, M., 2013. A low-cost electronic tensiometer system for continuous monitoring of soil water potential. J. Agric. Eng. *44* (3), 16. https://doi.org/10.4081/jae.2013.211.
Wang, S., An, J., Zhao, X., Gao, X., Wu, P., Huo, G., Robinson, B.H., 2020. Age- and climate- related water use patterns of apple trees on China's Loess Plateau. J. Hydrol. 582, 124462 https://doi.org/10.1016/j.jhydrol.2019.124462.
Wang, P., Song, X., Han, D., Zhang, Y., Liu, X., 2010. A study of root water uptake of crops indicated by hydrogen and oxygen stable isotopes: A case in Shanxi Province, China. Agric. Water Manag. *97* (3), 475–482. https://doi.org/10.1016/j.agwat.2009.11.008.
Wang, S., Zhao, X., Gao, X., Huo, G., Pan, Y., 2018. Water use source of apple trees with full productive age in less hilly region. Sci. Silvae Sin. 54 (10), 1001–7488. https://doi.org/10.11707/j.1001-748820181004.
Wang, L., Zhu, G., Qiu, D., Liu, Y., Zhao, K., Sang, L., Zhang, Z., Sun, Z., Yong, L., Jiao, Y., 2023. The use of stable isotopes to determine optimal application of irrigation-water to a maize crop. Plant Soil *482*, 679–696. https://doi.org/10.1007/s11104-022-05720-x.
Wen, M., He, D., Li, M., Ren, R., Jin, J., Si, B., 2022. Causes and factors of cryogenic extraction biases on isotopes of xylem water. Water Resour. Res. *58*, e2022WR032182 https://doi.org/10.1029/2022WR032182.
World Bank (2022). Water in agriculture. Available at: ⟨https://www.worldbank.org/en/topic/water-in-agriculture⟩.
Wu, Y., Du, T., Yuan, Y., Shukla, M.K., 2018. Stable isotope measurements show increases in corn water use efficiency under deficit irrigation. Sci. Rep. *8* (1), 14113 https://doi.org/10.1038/s41598-018-32368-4.
Wu, W., Tao, Z., Chen, G., Meng, T., Li, Y., Feng, H., Si, B., Manevski, K., Andersen, M.N., Siddique, K.H.M., 2022. Phenology determines water use strategies of three economic tree species in the semi-arid Loess Plateau of China. Agric. For. Meteorol. *312*, 108716 https://doi.org/10.1016/j.agrformet.2021.108716.
Zanotelli, D., Ben Abdelkader, A., Thalheimer, M., Brignach, A., Giuliani, N., Asensio, D., Andreotti, C., Tagliavini, M., 2022. Drivers of apple tree transpiration rates assessed by sap flow sensors. Acta Hortic. (*1373*), 19–24. https://doi.org/10.17660/ActaHortic.2023.1373.4.
Zhao, L., Gao, X., He, N., Zhao, X., 2022. Ecohydrological advantage of young apple tree-based agroforestry and its response to extreme droughts on the semiarid Loess Plateau. Agric. For. Meteorol. *321*, 108969 https://doi.org/10.1016/j.agrformet.2022.108969.
Zheng, L., Ma, J., Sun, X., Guo, X., Cheng, Q., Shi, X., 2018. Estimating the Root Water Uptake of Surface-Irrigated Apples Using Water Stable Isotopes and the Hydrus-1D Model. Water *10*, 1624. https://doi.org/10.3390/w10111624.
Zuecco, G., Amin, A., Frentress, J., Engel, M., Marchina, C., Anfodillo, T., Borga, M., Carraro, V., Scandellari, F., Tagliavini, M., Zanotelli, D., Comiti, F., Penna, D., 2022. A comparative study of plant water extraction methods for isotopic analyses: Scholander-type pressure chamber vs. cryogenic vacuum distillation. Hydrol. Earth Syst. Sci. *26*, 3673–3689. https://doi.org/10.5194/hess-26-3673-2022.